

CONF-9610742--4

LA-UR-96-4482

Title: DEVELOPMENT OF RECRYSTALLIZATION TEXTURE AND MICROSTRUCTURE IN COLD ROLLED COPPER

RECEIVED
FEB 14 1997
OSTI

Author(s): CARL T. NECKER, MST-6
ROGER D. DOHERTY, DREXEL UNIVERSITY
ANTHONY D. ROLLETT, CARNEGIE MELLON UNIVERSITY

MASTER

Submitted to: INCLUSION INTO CONFERENCE PROCEEDINGS
RECRYSTALLIZATION 1996 CONFERENCE ON
OCTOBER 21-24, 1996 AT MONTEREY, CA

DISTRIBUTION OF THIS DOCUMENT IS UNLIMITED

Los Alamos
NATIONAL LABORATORY

Los Alamos National Laboratory, an affirmative action/equal opportunity employer, is operated by the University of California for the U.S. Department of Energy under contract W-7405-ENG-36. By acceptance of this article, the publisher recognizes that the U.S. Government retains a nonexclusive, royalty-free license to publish or reproduce the published form of this contribution, or to allow others to do so, for U.S. Government purposes. The Los Alamos National Laboratory requests that the publisher identify this article as work performed under the auspices of the U.S. Department of Energy.

Form No. 836 R5
ST 2629 10/91

DISCLAIMER

**Portions of this document may be illegible
in electronic image products. Images are
produced from the best available original
document.**

DEVELOPMENT OF RECRYSTALLIZATION TEXTURE AND MICROSTRUCTURE IN COLD ROLLED COPPER

C.T. Necker*, R.D. Doherty**, A.D. Rollett***

*Los Alamos National Laboratory, MS G770, Los Alamos, New Mexico, 87545 USA

**Drexel University, Department of Materials Engineering, Philadelphia, Pennsylvania, 19104 USA

***Carnegie Mellon University, 5000 Forbes Avenue, Department of Materials Science and Engineering, 3327 Wean Hall, Pittsburgh, Pennsylvania, 15213-3890 USA

ABSTRACT

Oxygen free electronic copper, 99.995% purity, of two initial grain sizes, 50 μm and 100 μm , has been cold rolled to six strains of 1.0, 1.5, 2.0, 2.65, 3.5 and 4.5 (von Mises equivalents). The rolled materials were partially and fully recrystallized to study the development of recrystallization textures as a function of grain size, strain and fraction recrystallized. The initial textures were relatively random and the deformation textures show the classic β fiber development. As strain is increased both materials produce increasingly intense cube recrystallization textures, $\{100\}\langle 001\rangle$, as measured both by x-ray diffraction and the electron backscatter pattern (EBSP) techniques. The strong cube recrystallization textures are a product of a higher than random frequency of cube nucleation sites. An additional factor is that cube regions grow larger than non-cube regions. The explanation of the cube frequency advantage is based on the development of large stored energy differences between cube orientations and neighboring orientations due to recovery of cube sites. Of several possible explanations of the cube orientation size advantage, the most plausible one is solute entrapment. At the higher strains the boundaries of cube grains encounter the deformation texture S components, $\{123\}\langle 634\rangle$, changing the boundary character to one of $40^\circ\langle 111\rangle$. These boundaries are more resistant to solute accumulation than random high angle boundaries, allowing the boundaries to migrate with less of a solute drag effect than a random high angle boundary.

INTRODUCTION

It is well known that heavily cold rolled copper and warm/hot rolled aluminum, when recrystallized often produce strong cube textures, $\{100\}\langle 001\rangle$. The strength of the cube texture can be explained by the frequency and size of cube grains. Typically cube grains are defined as all those within 20° of the ideal cube orientation. Quantifying the frequency and size of grains has been made easier with the advent of the automated methods of measuring texture on a microscopic scale (1). Local texture measurements are made over an matrix of points on a sample surface. Microstructure information is derived from this matrix of orientations by applying boundary criteria to the misorientation between

every point and its neighboring points. The misorientation criteria define the minimum misorientation which delineates regions that have developed from different nucleation events. Typically the minimum misorientation criteria is set at 15°. However, in the case of very strong cube recrystallization textures it is likely that cube grains grow to impingement on each other with misorientations less than 15°. It has been shown in both aluminum and copper that a misorientation criteria of 2° is necessary to fully delineate the EBSP microstructure in recrystallized materials dominated by the cube texture (2,3).

The microstructure information derived from microtexture measurements provides insight as to the impact of frequency and size on the development of strong cube textures. The relative impacts are quantified by simple ratios as shown by Doherty (4). Frequency and size parameters, α and β respectively, are defined as follows.

$$\alpha = f_c/f_r \quad (1)$$

$$\beta = d_c/d_{nc} \quad (2)$$

f_c is the frequency of cube grains in the recrystallization texture and f_r is the frequency of cube grains one would expect in a random texture. d_c and d_{nc} are respectively the average grain sizes of cube and non-cube grains. If $\alpha > 1$ then the frequency of cube grains is greater than one would expect from a random texture. If $\beta > 1$ then the average cube grain is larger than the average non-cube grain. In a series of investigations of strong cube textures in aluminum alloys, Hjelen et al. (5), Doherty et al. (6), Samajdar (7), Vatne (8) and Daaland and Nes (9) find $\alpha \gg 1$ and $\beta \approx 1$. Several investigators have found $\beta > 1$ in weak cube textures, Juul Jensen et al. (10), Hjelen et al. (5). Juul Jensen and coworkers found for 90% cold rolled commercial purity aluminum that $\alpha < 1$ and $\beta \approx 2.3$.

In light of these results, the development of cube textures in high purity copper is investigated to determine if the frequency and size parameters found in the copper are similar to those found in aluminum. An explanation of frequency and size advantages is developed based on mechanisms known to affect to development of recrystallization textures.

PROCEDURE

Two one inch thick plates of oxygen free electronic copper (Table 1 lists impurities), 50 μm and 100 μm grain sizes, were unidirectionally cold rolled to reductions, 58%, 73%, 82%, 90%, 95% and 98% (strains of 1.0, 1.5, 2.0, 2.65, 3.5 and 4.5 von Mises). 1 cm x 1.5 cm samples were cut from the rolled sheets and recrystallized in a silicon oil bath at temperatures allowing the material to fully recrystallize between 0.5 and 1 hour. Partially and fully recrystallized samples were mounted on their long transverse edge and metallographically prepared. The mechanically polished surface was then electropolished in a 50/50 solution of phosphoric acid.

Table 1. Material Compositions—nominally 99.995% purity for 50 μm and 100 μm materials in ppm.

Impurity -->	O	Ag	S	P	Te	Fe	Sb	Sn	Ni	Other
50 μm	7	<0.5	6	<2	6	5	3	4	4	13
100 μm	7	5	10	<2	3	5	3	2	4	14

EBSP textures were measured on this surface using automated microtexture systems on a ElectroScan environmental scanning electron microscope and a Philips field emission gun scanning electron microscope. The matrix of orientations was measured in 10 μm steps over a 1 mm distance in the rolling direction, from the sample surface to the centerline. The orientation and image quality of each point was recorded. The image quality refers to the quality of the electron backscatter pattern which,

in turn, is a function of the distortion of the atomic lattice. Strained material produces relatively low image qualities while recrystallized material produces relatively sharp, strong patterns, yielding high image qualities.

Microstructure information was derived from the texture data by applying a 2° misorientation criteria to delineate grains of different nucleation events. The precision of orientation measurements is less than 1° so the 2° criteria does not introduce artificial boundaries. Cube grains are defined as those with orientations within 20° of $\{100\}\langle 001\rangle$. All other grains are categorized as non-cube. An added complexity in determining the influence of frequencies and sizes of grains on the recrystallization texture is the presence of annealing twins. To properly evaluate the development of cube textures the cube volumes within cube grains were separated from the cubetwin volumes. As an example, a cube grain may be composed of two cube regions (zones) separated by an annealing twin. This grain contains three different zones, one nucleated from the deformed structure and the other two, through the twinning process. The extent of the cube volume is dependent on the number of cube zones, not the number of cube grains, and the extent of growth of these zones. Calculation of grain frequencies and sizes uses a misorientation criteria of $60^\circ\langle 111\rangle \pm 5^\circ$ to couple related twins to their parent orientations.

EXPERIMENTAL RESULTS AND DISCUSSION

The selected pole figures in Figure 1 show that both materials develop strong cube recrystallization textures with increasing strain.

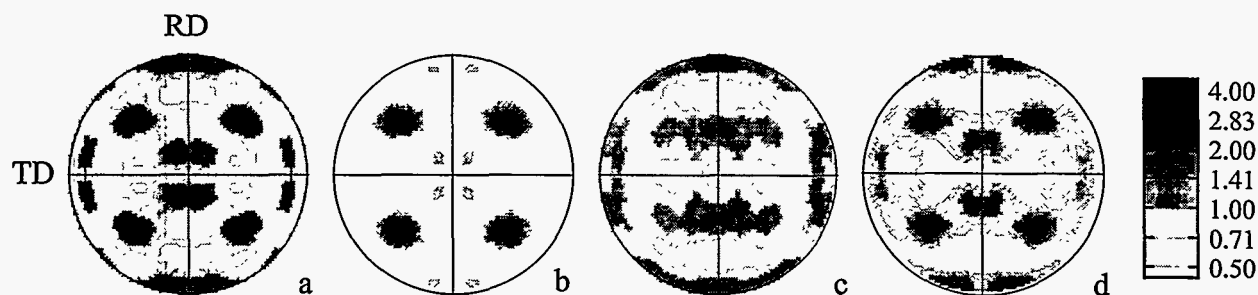


Figure 1. 111 x-ray pole figures of copper fully recrystallized after rolling. 50 μm material: a) $\epsilon=2.0$, b) $\epsilon=4.5$, 100 μm material: c) $\epsilon=2.0$, d) $\epsilon=4.5$

The cube volumes, defined by 5° , 10° , 15° and 20° misorientations from ideal cube, are shown in Figure 2. Not only does the volume of cube increase significantly but the cube texture becomes sharper, more closely aligned with ideal cube. Assuming that cube zones nucleate from cube bands in the deformed structure, this result suggests that there is near-ideal cube oriented material in the deformed structure. Duggan et al. (11) show that cube oriented bands exist in the deformed structure in heavily rolled copper.

The source of the recrystallized cube volume increase is either due to an increased frequency of cube zones and/or the larger than average size of cube zones as compared to non-cube zones. Figure 3 shows that the number of cube zones increases as a function of strain while there is little change in the number of non-cube zones.

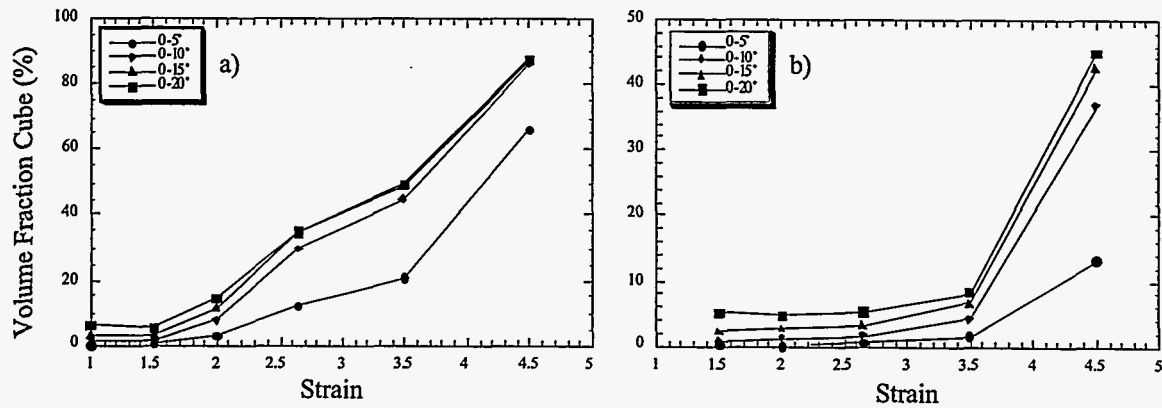


Figure 2. Cube volume as a function of strain in fully recrystallized materials: a) 50 μm and b) 100 μm copper.

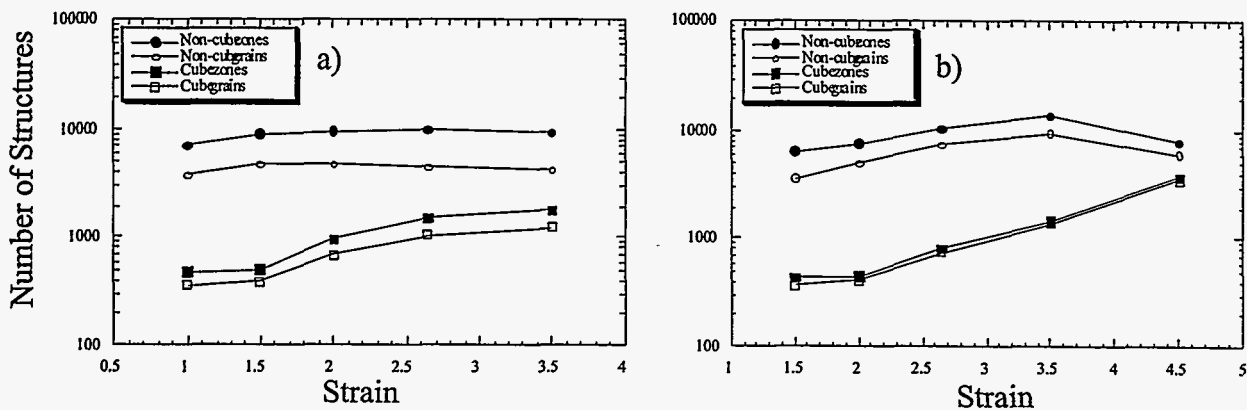


Figure 3. Number of recrystallized cube and non-cube grains and zones as a function of strain: a) 50 μm and b) 100 μm copper.

When these absolute values are combined as the α parameter, it is readily seen that α increases with strain, Table 2.

Table 2. α parameter for cube oriented material as a function of strain for 50 μm (fg) and 100 μm (cg) materials. Parameter is defined for cube grains and cube zones.

strain	fg α (grains)	fg α (zones)	cg α (grains)	cg α (zones)
1.0	1.82	1.41	-	-
1.5	1.64	1.18	1.93	1.30
2.0	2.64	2.11	1.59	1.16
2.65	3.97	3.23	1.93	1.53
3.5	4.81	4.12	2.67	2.02
4.5	-	-	7.94	6.83

At all strains the frequency of cube zones is greater than one would expect from a random texture. It should be kept in mind that the frequency of cube zones is a function of how many cube grains nucleate from the deformed structure and how many additional cube zones are formed by twinning. The increased frequency of cube grains indicates that the number of active cube nucleation sites within the deformed structure increases with strain. The activation of sites for growth is subject to the presence of sufficiently high local stored energy differences spanning mobile boundaries. So the

increased frequency occurs because either the stored energy difference between cube sites and neighboring sites increases with strain and/or the boundaries between cube and neighboring sites possess greater mobilities at higher strains. Duggan et al. (11) found that cube sites are often neighbored by S oriented deformation bands, $\{123\}\langle 634\rangle$, and preferentially grow in the S bands. Their explanation of the preferential nucleation is based on micro-growth selection. The cube and S orientations are misoriented by approximately $40^\circ\langle 111\rangle$. It is suggested that the higher initial mobility of this boundary allows cube grains to nucleate readily. The sharpening cube texture coupled with the increasing volume and sharpness of S oriented bands with increasing strain provides a mechanism for formation of $40^\circ\langle 111\rangle$ boundaries.

Samajdar (2), while investigating warm rolled commercial purity aluminum, found that deformed cube regions were likely to grow into S oriented bands as well as most any other deformation texture component. Transmission electron microscopy on the deformed material showed that there was a significant difference in the dislocation density between cube and other deformed regions with cube being more strain free than any other orientation in the deformed structure. The largest difference was found to be between cube and S. Samajdar suggests that it is the large stored energy difference between cube and S as well as other deformed orientations that is responsible for the increased frequency of cube grains.

A 95% rolled, 9% recrystallized copper sample has been characterized using a high resolution electron microscope (Carnegie Mellon University) to reveal the deformed and recrystallized textures via EBSP. When fully recrystallized, this sample produces a cube volume of about 60%. Figure 4 shows the orientation map with boundaries $> 2^\circ$ and cube related regions shaded dark.

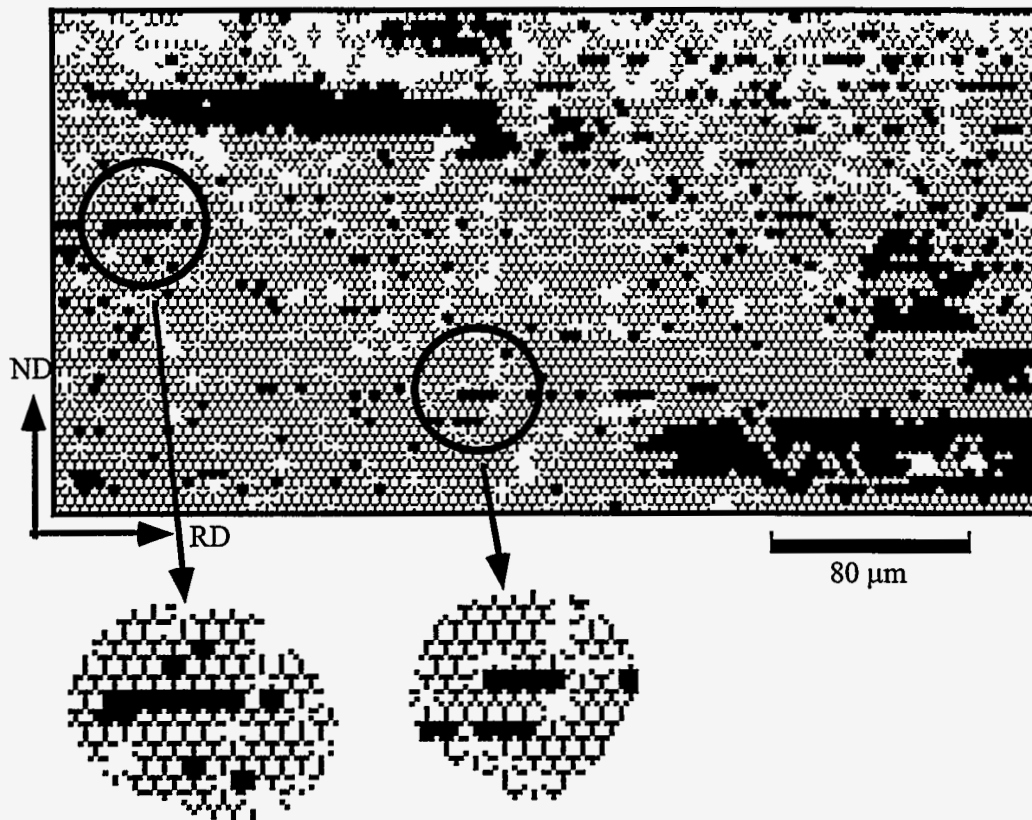


Figure 4. Number of recrystallized cube and non-cube grains and zones as a function of strain: a) 50 μm and b) 100 μm copper.

The significant features are the presence of large recrystallized cube grains which show almost no internal misorientations and thin, shorter cube bands containing internal misorientations every 4 μm (resolution of the microtexture scan). The image quality parameter of the recrystallized cube grains is on average about 150 whereas that of the deformed material is about 40. Many of the cube bands, such as the one circled in the middle of the frame, have image qualities between 60 and 80. Some of these cube bands must become active nucleation sites if the texture is to eventually become 60% cube. The higher average image qualities within these bands suggests that the cube regions have undergone recovery, allowing the image quality to increase above that characterizing the deformed microstructure. Ridha and Hutchinson (12) found that cube recovers more easily than other orientations in cold rolled copper. These findings support the theory of the Ridha and Hutchinson that cube oriented regions recover more easily due to minimal elastic interactions of dislocations having orthogonal Burgers vectors. The lack of misorientations within the recrystallized cube grains indicates that the misorientations within the cube bands must be removed as part of the recovery or recrystallization process. Boundaries surrounding the cube bands with higher image quality values are not characterized as $40^\circ\langle 111 \rangle$ boundaries. These findings support the suggestion that cube nucleation frequency increases due to the increasing stored energy difference between recovered cube regions and less recovered (or not recovered at all) non-cube regions. These authors however do not discount the possibility that the frequency advantage may also be aided by the formation of higher mobility boundaries, whether they have higher mobilities due to solute accumulation resistance or simply that the boundary possesses low concentrations of solute at the initiation of growth. These boundaries are also characterized as low energy boundaries, reducing the energy necessary to activate boundary migration. This is an area of future investigations.

The average size of recrystallized cube and non-cube zones as a function rolling strain is plotted in Figure 5. The 50 μm copper (a) shows an increase in cube zone size and a decrease in the non-cube zone size. The 100 μm copper (b) shows a decrease in both cube and non-cube zones sizes and then an increase in cube zone size while the non-cube zone size continues to decrease.

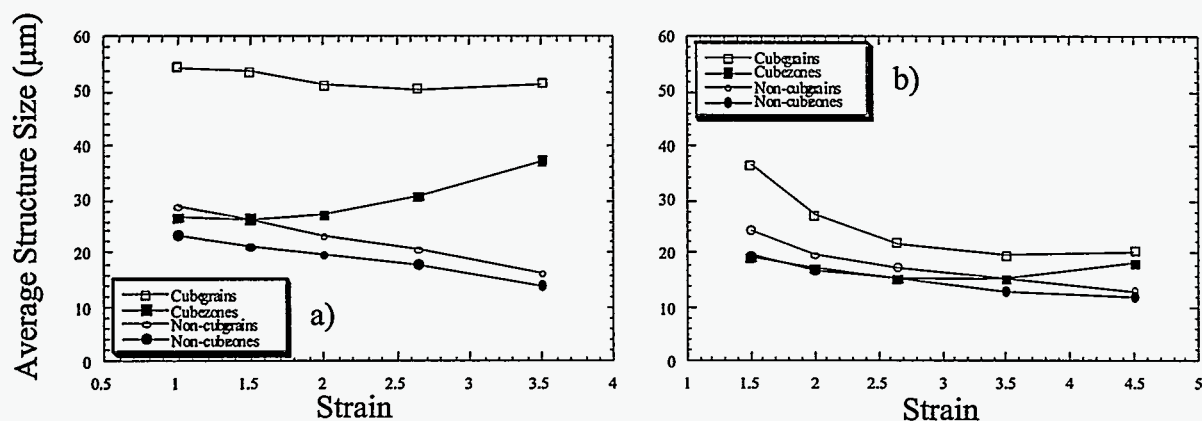


Figure 5. Average size of recrystallized cube and non-cube grains and zones as a function of strain: a) 50 μm and b) 100 μm copper.

Table 3 presents the β parameters for grain and zone sizes. In the 50 μm copper $\beta > 1$ at all strains for cube zones. In the coarse grain copper $\beta \approx 1$ at lower strains and then becomes $\beta > 1$ at higher strains.

Table 3. β parameter for cube oriented material as a function of strain for 50 μm (fg) and 100 μm (cg) materials. Parameter is defined for cube grains and cube zones.

strain	fg β (grains)	fg β (zones)	cg β (grains)	cg β (zones)
1.0	1.89	1.15	-	-
1.5	2.05	1.25	1.51	.98
2.0	2.21	1.39	1.39	1.03
2.65	2.46	1.72	1.26	1.01
3.5	3.19	2.67	1.3	1.17
4.5	-	-	1.56	1.59

As stated earlier, most of the investigations of aluminum derive $\beta \approx 1$ for strong cube recrystallization textures with several instances where $\beta > 1$, Juul Jensen et al. (10), Hjelen et al. (5) and Daaland and Nes (9). Juul Jensen and co-workers suggested that cube grains grew more rapidly than randomly oriented grains. Hjelen et al. suggested that the β factor was due to a less than competitive growth environment (many cube grains and few non-cube grains). Daaland and Nes explained the larger than average cube grains based on the relative rates of recrystallization and precipitation. When the material precipitated in advance of recrystallization the cube grains grew larger than average whereas if precipitation was avoided cube grains were the same size as other grains. Although speculative, and currently without experimental support, it is suggested that the $\beta > 1$ is due to the degree to which advancing cube boundaries interact with solute. The following scenario has been developed to explain $\beta > 1$ in high purity copper and $\beta \approx 1$ and $\beta > 1$ in aluminum alloys. As most boundaries advance through the deformed material they accumulate solute, decreasing the boundary mobility. Growing cube zones (grains in aluminum) occasionally encounter S oriented bands thereby changing the boundary character to that of near $40^\circ \langle 111 \rangle$. When this happens the boundary continues to grow through the S orientation while accumulating solute at a slower rate or not at all or maybe even losing solute. Which ever the effect, the boundary grows a certain distance without increasing the solute drag effect that other boundaries would sense over the same growth distance. This type of effect is likely to be more effective at higher strains as the cube-S interactions become more probable. In all cases where $\beta > 1$ in aluminum alloys the aluminum is either a high purity aluminum or a commercial purity aluminum which has undergone precipitation. Aluminum alloys not precipitated present a deformed matrix heavily laded with solute such that formation of $40^\circ \langle 111 \rangle$ boundaries may not have a significant impact on the solute drag effect. The purification of the aluminum deformed matrix by precipitation makes the aluminum more like the copper case where the solute accumulation effect develops more slowly. It is suggested that these theories be tested by cold rolling zone refined aluminum to determine if low alloy content aluminum shows $\alpha > 1$ and $\beta > 1$.

CONCLUSIONS

The annealing of heavily cold rolled of high purity copper produces strong cube recrystallization textures. The volume fraction cube increases with increasing strain as does the sharpness of the cube texture. The strong cube texture development occurs because the frequency of cube zones, nucleated both from the deformed structure as well as by twinning, increases with increasing strain. The development is also aided by an increasing size differential between cube and non-cube zones.

The increasing frequency of cube sites is explained by a stored energy differential theory. It is suggested that cube recovers more readily than other orientations, developing a large stored energy differential with the neighboring orientations. Direct evidence by transmission electron microscopy is still needed as well as a statistical information concerning nearest neighbors to cube deformation bands.

The increasing cube zone size is speculatively explained by the increasing occurrence of cube growth sites interacting with S oriented deformation bands. The boundary between cube and S orientations are more resistant to solute accumulation than random high angle boundaries. The slower rate of solute accumulation allows the cube zones to grow larger than non-cube zones.

ACKNOWLEDGMENTS

The authors wish to thank H. Garmestani and the National High Magnetic Field Laboratory for the use of their EBSP system. Additional thanks is extended to Carnegie Mellon University for the use of their field emission gun EBSP system.

REFERENCES

1. Wright, S.I., B.L. Adams and K. Kunze (1993). *Mater. Sci. Eng.*, **A160**, 229.
2. Samajdar, I. (1994). Ph.D. Thesis, Drexel Univerisity, Philadelphia, Pennsylvania.
3. Necker, C.T. (1996). Ph.D. Thesis, Drexel Univerisity, Philadelphia, Pennsylvania.
4. Doherty, R.D. (1985). *Scripta Met.*, **19**, 927.
5. Hjelen, J., R. Ørsund and E. Nes (1991). *Acta Metall.*, **39**, 1377.
6. Doherty, R.D., K. Kashyap and S. Panchanadeeswaran (1993). *Acta Metall.*, **41**, 3029.
7. Samajdar, I. and R.D. Doherty (1995). *Scripta Met.*, **32**, 845.
8. Vatne, H.E. (1995). Ph.D. Thesis, University of Trondheim, Norway.
9. Daaland, O. and E. Nes (1995). *Acta Metall.*, **44**, 1413.
10. Juul Jensen, D., N. Hansen and F.J. Humphreys (1985). *Acta Metall.*, **33**, 2155.
11. Duggan, B.J., K. Lücke, G.D. Köhlhoff and C.S. Lee (1993). *Acta Metall.*, **41**, 1921.
12. Ridha, A.A. and W.B. Hutchinson (1982). *Acta Metall.*, **30**, 1929.

DISCLAIMER

This report was prepared as an account of work sponsored by an agency of the United States Government. Neither the United States Government nor any agency thereof, nor any of their employees, makes any warranty, express or implied, or assumes any legal liability or responsibility for the accuracy, completeness, or usefulness of any information, apparatus, product, or process disclosed, or represents that its use would not infringe privately owned rights. Reference herein to any specific commercial product, process, or service by trade name, trademark, manufacturer, or otherwise does not necessarily constitute or imply its endorsement, recommendation, or favoring by the United States Government or any agency thereof. The views and opinions of authors expressed herein do not necessarily state or reflect those of the United States Government or any agency thereof.
